iScience

Article

Magnetic responses for heavy metal pollution recorded by the sediments from Bohai Sea, Eastern China

Xiaohui Wang,
Longsheng Wang,
Shouyun Hu, ...,
Chao Zhan,
Xianbin Liu, Qing
Wang

52wls@163.com (L.W.)
hu_shouyun@hotmail.com
(S.H.)

Highlights

A series of magnetic
parameters of the
sediments from Bohai Sea
was established

The predominant
magnetic minerals of
Bohai Sea sediments were
magnetite

There is positive
relationship between
magnetic parameters and
heavy metals

The environmental
implications of the Bohai
Sea were successfully
reconstructed

iScience

Article

Magnetic responses for heavy metal pollution recorded by the sediments from Bohai Sea, Eastern China

Xiaohui Wang,[1] Longsheng Wang,[1,2,3,4,5,*] Shouyun Hu,[4,*] Liwei Meng,[1] Lin Zeng,[1] Buli Cui,[1] Chao Zhan,[1] Xianbin Liu,[1] and Qing Wang[1]

SUMMARY

The Bohai Sea is facing multidirectional pressure from economic development and pollutant emissions. Magnetic minerals and heavy metal concentrations in the sediments of core M5 from the Bohai Sea were performed. The results of concentration-related magnetic parameters, heavy metal contents, and PLI (Tomlinson pollution load index) illustrate there are essential linkages of the sources, migration, and deposition. The predominant magnetic mineral was magnetite. Based on the chronological data from ^{210}Pb and ^{137}Cs activities, the increasing magnetic parameters and heavy metal concentrations at a depth of 81 cm were dated to 1950 CE, which corresponded to the establishment of the People's Republic of China; the decrease at depths of 37–45 cm and 16–18 cm may be related to the decline in steel production in 1960 CE and the Tangshan earthquake in 1978 CE, respectively. This study enriches relevant theories of environmental magnetism via the ecological and environmental protection of the coastal zones.

INTRODUCTION

Environmental magnetism is a new frontier subject between earth science, magnetism, and environmental science (Thompson et al., 1980). By studying the migration, transformation, and combination of magnetic minerals in environmental systems, environmental magnetism explores the effects, problems, and influences of human activities at different spatial and temporal scales and reveals the process and mechanism of environmental changes according to the relationship between magnetic properties and the reflected environmental connotation (Liu et al., 2012). When studying heavy metal pollution, environmental magnetism mainly focuses on determining the pollution scope, describing the pollution degree, tracing pollution sources, analyzing the magnetic parameters, and separating the magnetic information from natural and human-made sources (Dong et al., 2014; Yu and Lu, 2016; Wang et al., 2018a; 2018b).

One focus of the environmental magnetic monitoring of heavy metal pollution is analytical semiquantification and method standardization. The potential processes and the relationships between magnetic minerals and heavy metal concentrations can be better understood by investigating different environmental pollution situations. Previous studies covered heavy metal pollution monitoring in cities (Li et al., 2014), atmospheric control of pollutant diffusion (Wang et al., 2019), hydrological monitoring of pollutant transport (Mariyanto et al., 2019), and characteristics of anthropogenic spherules (Zhu et al., 2012). Another focus of this field is to accurately understand the response mechanism of heavy metal pollution, evaluate the environmental pollution status, and analyze the multistructure heavy metal pollution sources (Bandaru et al., 2016; Wang et al., 2018a; 2018b). Many studies have been focused on high-resolution magnetic scanning and monitoring of a variety of sediments, which makes up for the blindness of chemical analysis and is gradually becoming a new development direction in current ecological environment monitoring, especially heavy metal monitoring.

The Bohai Rim region, located in the center of Northeast Asia with a coastline of more than 5,800 km, is the third economic growth pole after the economic circle of the Yangtze and Pearl River deltas (Cui, 2015). Coupled with the rapid socioeconomic development of the Bohai Rim region and the hastening of urbanization, the urban sewage, untreated industrial waste water, pesticides, and fertilizers have been directly discharged into the Bohai Sea, greatly affecting its ecological environment to become a sewage pool.

[1]Coast Institute of Ludong University, Yantai 264025, China

[2]Key Laboratory of Coastal Environmental Processes and Ecological Remediation, Yantai Institute of Coastal Zone Research (YIC), Chinese Academy of Sciences (CAS), Yantai 264003, China

[3]State Key Laboratory of Loess and Quaternary Geology, Institute of Earth Environment, Chinese Academy of Sciences, Xi'an 710061, China

[4]State Key Laboratory of Lake Science and Environment, Nanjing Institute of Geography and Limnology, Chinese Academy of Sciences, Nanjing 210008, China

[5]Lead contact

*Correspondence:
52wls@163.com (L.W.),
hu_shouyun@hotmail.com (S.H.)
https://doi.org/10.1016/j.isci.2022.105280
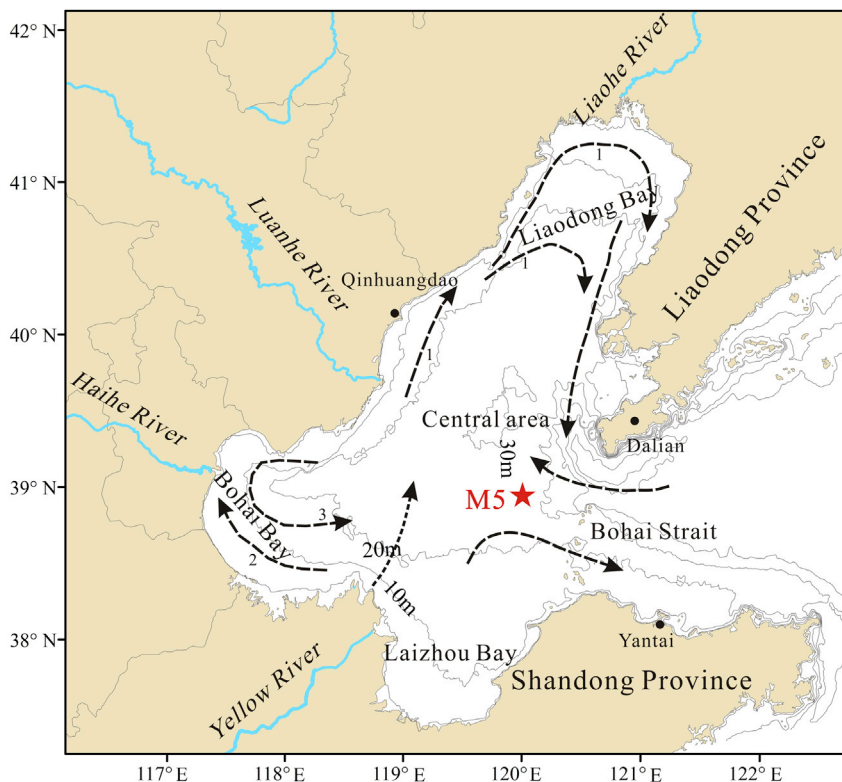
Figure 1. The study area and location of sampling sites in the Bohai Sea
General current circulation system was modified from Zhao et al. (1995) and Qiao et al. (2010) ((1-clockwise circulation in the Liaodong Bay; 2, 3-*anti*-clockwise and clockwise circulation in the northern and southern Bohai Bay)).

Statistics show that the pollutants discharged into the Bohai Sea amount to more than 7×10^5 t every year—nearly half of the total sea pollutants nationwide (Xu et al., 2013). Therefore, it is imperative to strengthen the relevant heavy metal pollution research in the Bohai Sea and explore a rapid, sensitive, economical, and nondestructive method to conduct large-scale pollution investigation. Moreover, the sediments of the Bohai Sea are continuous and undisturbed, making it an ideal location to reconstruct heavy metal history using magnetic parameters. The objectives of this study were to (1) identify the relationship between magnetic parameters and heavy metals, (2) reconstruct quantitatively the heavy metal history in Bohai sea, and (3) discuss the environmental implications of magnetic minerals and heavy metals.

The Bohai Sea in Northeast China is a nearly enclosed inland sea that comprises three bays and a central sea. The three bays are Bohai Bay in the west, Laizhou Bay in the south, and Liaodong Bay in the north. The Bohai Sea is connected to the north Yellow Sea in the east by the Bohai Strait (Figure 1). The total area of the Bohai Sea is approximately 7.7×10^4 km^2, with a water volume of 1.7×10^3 km^3. Human population is approximately 7×10^7 in the Bohai Sea coastal area. The average water depth of the Bohai Sea is 12.5 m, with a maximum water depth of 70 m near the northern shore of the Bohai Strait (Gao et al., 2014). More than 40 rivers flow into the Bohai Sea, with the Yellow, Luanhe, Liaohe, and Haihe rivers being the four major ones (Figure 1). The amount of particulate matter imported from the coastal rivers into the Bohai Sea is $\sim 1.3 \times 10^9$ t/yr (Chen and Wang, 1996; Liu et al., 2007). With rapid economic and social development around the Bohai Sea Rim, the heavy metal pollutants flowing into the Bohai Sea are increasing significantly, thereby rapidly deteriorating its environmental quality. Bulletins have indicated that the polluted areas of the Bohai Sea in 2011 total 4,210 km^2. The polluted areas in 2012 and 2013 were 13,080 and 8,490 km^2, respectively, which were significantly larger than that in 2011 (State Oceanic Administration of China, 2014).

Core M5 (a water depth of 22 m, located at 39°5.58′ N, 120°0′ E) was collected using a vibracoring system in the central basin of the Bohai Sea in June 2018 (Figure 1). Inspection of the core M5 indicated that the sediment–water interface was restored at the time of sample collection. The sections of core M5 were
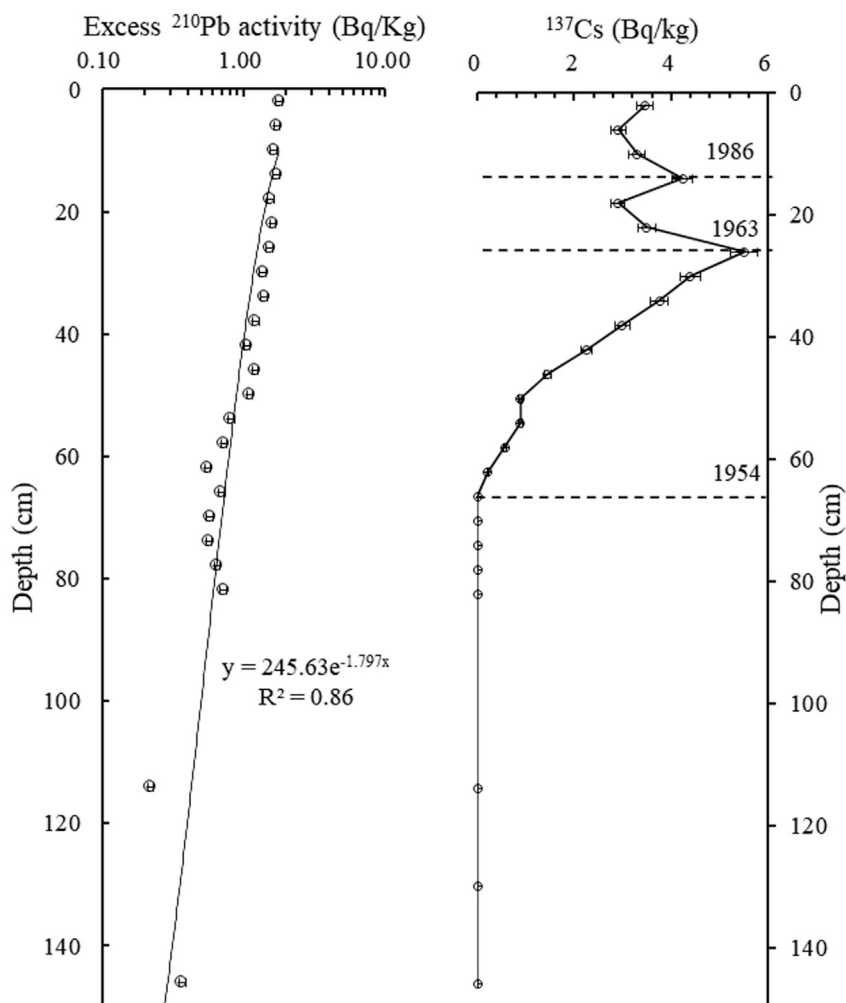
Figure 2. Profiles of excess ^{210}Pb activity and ^{137}Cs in core M5 from Bohai Bay

segmented, photographed, and visually described in the laboratory. The total penetration depth of core M5 was 337 cm. In this study, we mainly discuss the magnetic properties of heavy metal concentrations of a segment of the core between 0 and 150 cm. All the samples were collected into numbered plastic bags and placed in a refrigerator at 4°C prior to analysis.

RESULTS

Age–depth model of core M5

Radiometric ^{210}Pb and ^{137}Cs were used to provide the age chronologies between 0 and 150 cm of core M5 (Figure 2). The ^{210}Pbexc of core M5 at the bottom of the sample at a depth of 1 cm was 4.08 Bq/kg, which decreased to 0.35 Bq/kg at a depth of 145 cm. The average sedimentation rate based on the ^{210}Pbexc activity was calculated to be 0.99 cm/yr. However, the ^{210}Pb sedimentation rate is often influenced by a mixing affect in the coastal zones (Zhou et al., 2021). Therefore, ^{137}Cs was used for age calculation. Based on the two peaks (1986 and 1963 CEs) at depths of 14 and 26 cm, respectively, we determined the sedimentation rate to be 0.43 cm/yr between 1986 and 2018 CE and 0.52 cm/yr between 1963 and 1986 CE. The ^{137}Cs activity reduced to zero at a depth of 66 cm, which corresponded with the fallout of 1954 CE (Leslie and Hancock, 2008; Zhou et al., 2021). The sedimentation rate during 26–66 cm was calculated at 4.44 cm/yr. Since 1963 CE, the reduction in sedimentation rate was possibly related with a decrease in the sediment flux from the Yellow River into the Bohai Sea (Wang et al., 2017a; Wang et al., 2017b). Based on the sedimentation rates of core M5, the bottom layer during 0–150 cm of core M5 was dated to around 1930 CE, enabling us to reconstruct the environmental changes of Bohai Sea over the last 90 years.
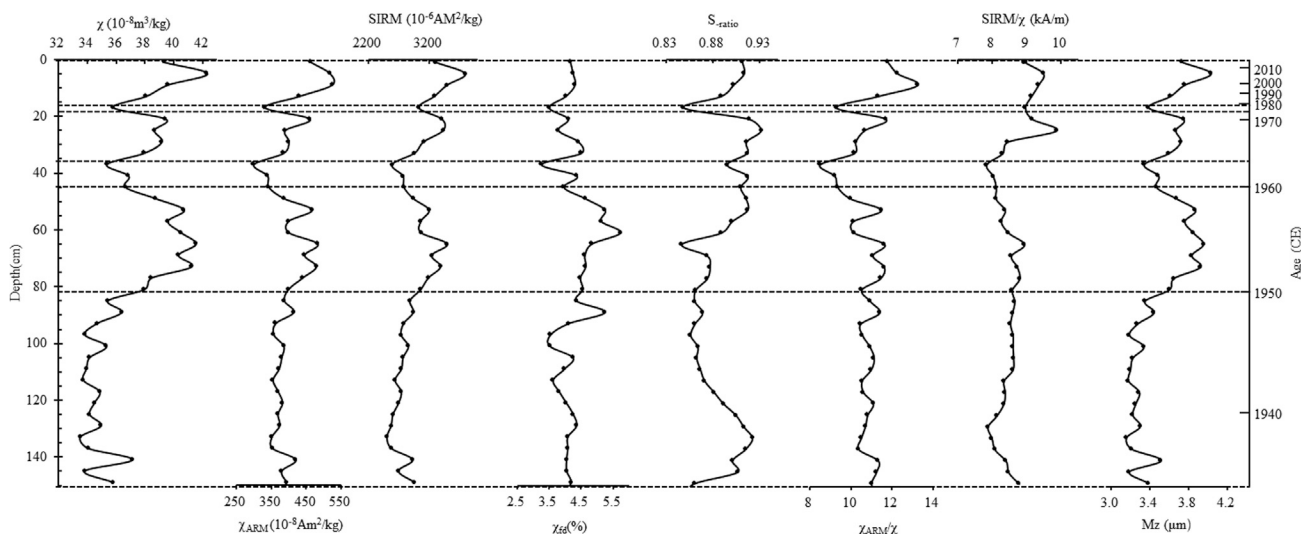
Figure 3. Vertical variation of magnetic parameters and grain size of core M5 from the Bohai Sea

Variation of magnetic parameters and grain size

The χ and SIRM values can reflect variations in the magnetic-mineral concentrations, especially ferro(i)magnetic minerals such as magnetite. The χ values of core M5 range from 33.53 to 42.33 × 10^{-8} m^3/kg with a mean of 36.94 × 10^{-8} m^3/kg. The variations in SIRM were similar to χ, which ranged from 2510.29 to 3804.23 × 10^{-6} Am^2/kg with a mean of 2985.81 × 10^{-6} Am^2/kg. The χ_{ARM} values mainly reflect the variations in single-domain (0.01–1 μm) and pseudo-single-domain (PSD) (1–10 μm) magnetic particles. The χ_{ARM} values of core M5 varied from 300.54 to 524.62 × 10^{-8} m^3/kg, with a mean value of 399.72 × 10^{-8} m^3/kg. The χ, SIRM, and χ_{ARM} values increased at a depth of 81 cm and obviously decreased depths of 37–45 and 16–18 cm. The values of χ_{fd}% varied from 3.27 to 5.74 with a mean of 5.27, which demonstrated the important contribution of superparamagnetic minerals. S_{-ratio} values can be used to indicate the relative proportion of soft and hard magnetic minerals. The S_{-ratio} values of core M5 ranged from 0.85 to 0.93 with a mean of 0.89, indicating that soft magnetic minerals were important magnetic constituents. Mean grain size (Mz) values range from 3.15 to 4.03 μm, with a mean of 3.51 μm. The changes of Mz are consistent with the results of χ and χ_{ARM}/χ (Figure 3).

Concentration of heavy metals

The concentration of heavy metals in core M5 of the Bohai Sea are presented in Figure 3 and Table 1, with averages that present wide variation: Fe (1.17%–1.61%), Ni (20–30 mg/kg), Cu (17–28 mg/kg), Zn (49–77 mg/kg), and Pb (16–26 mg/kg). Heavy metal content increased at a depth of 81 cm and decreased at depths of 37–45 and 16–18 cm, which was similar to the changes in χ, SIRM, and χ_{ARM}. Meanwhile, the heavy metal content of Fe, Ni, Cu, Zn, and Pb of river sediments in the Yellow, Liaohe, Luanhe, and Haihe rivers is also given in Table 1 (Chen and Wang, 1996; Liu et al., 2007). The average Fe, Ni, Cu, Zn, and Pb concentrations of sediments of core M5 were significantly lower than the background values of river sediments, which may be caused by heavy metals dissolved in water (Li and Zhang, 2010). Furthermore, the variations in PLI are similar to the variations in χ, χ_{ARM}, and SIRM values (Figure 4).

High-temperature κ–T and magnetic hysteresis loop curves

High-temperature κ–T curves can effectively identify magnetic minerals. During the process of heating and cooling, magnetization and magnetic susceptibility can show different characteristics with temperature change. These characteristics can often reflect the phase transition and Curie temperature (Tc) of different magnetic minerals, which can identify the types of magnetic minerals in samples (Thompson and Oldfield, 1986; Wang et al., 2017a, 2017b). All the heating curves of samples of core M5 indicated a Tc of 580°C, showing that magnetite was the dominant magnetic mineral. The κ–T curves could not decrease to zero after 580°C, indicating that hard magnetic minerals such as hematite may exist. The magnetic susceptibility of the cooling curve was higher than that of the heating curve, indicating the formation of ferro(i)magnetic minerals during the heating process (Wang et al., 2018a, 2018b) (Figure 5). In addition, the magnetic

Table 1. Concentration of geochemical elements of core M5 in Bohai Sea and the comparison to the background values in the coastal river sediments

Geochemical elements	The sediments of core BHB15 in the Bohai Sea			Backgraound values in the Luanhe River	Background values in the Haihe River	Background values in the Yellow River	Background values in the Liaohe River
	Min	Max	Mean				
Fe (%)	1.17	1.61	1.37	3.85	4.12	3.55	3.15
Ni (mg/kg)	20	30	24.05	37.1	44.1	42.1	38.2
Cu (mg/kg)	17	28	20.84	11	41	27	56.7
Zn (mg/kg)	49	77	57.47	35	139	78	151.5
Pb (mg/kg)	16	26	19.82	23.8	23.1	20.9	30

susceptibility of sample 70 fluctuates slightly near 400°C, which may be related to the transformation of iron-containing silicate into strong magnetic minerals during heating (Deng et al., 2000) (Figure 5).

When magnetic minerals are magnetized in an external magnetic field, the change in magnetization intensity will lag behind changes in the intensity of the external magnetic field, which can effectively reflect the soft and hard magnetic components as well as particle size of magnetic minerals in samples (Thompson and Oldfield, 1986; Liu et al., 2012). As shown in Figure 4, the magnetic hysteresis loop is thin, closed, and close to magnetic saturation below 300 mT. The loop also shows a low-coercivity behavior, indicating that the magnetic minerals are mainly soft ferromagnetic minerals. Furthermore, the low Bc (8.19–9.28 mT) and M_{rs}/M_s (0.106–0.124) values also indicated that soft-ferro(i)magnetic minerals were the dominant magnetic minerals (Figure 5).

DISCUSSION

Characteristics of magnetic minerals of core M5

The values of S$_{-ratio}$, high-temperature κ–T curves, and magnetic hysteresis loop curves demonstrated that the magnetic minerals of the assemblages of core M5 were dominated by magnetite. Previous studies have shown that SIRM/χ values can be used to identify the characteristics of magnetic minerals, as different magnetic minerals have different SIRM/χ values, such as magnetite with 11 kA/m, hematite with 261 kA/m, and pyrrhotite with 206 kA/m (Peters and Dekkers, 2003; Wang et al., 2019). The SIRM/χ values of sediments in core M5 from the Bohai Sea ranged from 7.33 to 9.38 kA/m with a mean of 8.06 kA/m, which was similar to the SIRM values of magnetite. Additionally, the low-SIRM/χ values indicated that the predominant magnetic minerals were magnetite with no formation of secondary magnetic minerals. The Pearson's correlation coefficients between χ as well as χ_{ARM} and SIRM are significant (R^2 = 0.81–0.88), which indicated that ferro(i)magnetic minerals contribute significantly to the magnetism of sediments of core M5. These results conflict with the results of χ_{fd}%, showing that there may be some outer core of the oxide magnetite particles, which are mainly part of the oxide magnetite particles (Sagnotti and Winkler, 2012). The grain size of the magnetic minerals is greater than 2 μm, as suggested by King plots (King et al., 1982) (Figure 6), implying that magnetic minerals are dominated by multidomain (MD) and PSD magnetite. A semiquantitative mixing model using χ_{fd}% and χ_{ARM}/SIRM values can effectively show the magnetic-mineral grain size (Dearing et al., 1996). The χ_{fd}% and χ_{ARM}/SIRM values of sediments in core M5 from Bohai Sea also fall at MD and PSD (Figure 6).

The primary principle that needs to be clarified when using magnetic parameters to monitor heavy metal pollution is the origin of the magnetic minerals in the sediments. When magnetic minerals in the sediments are determined to be predominantly magnetite, possible sources of the magnetic minerals include both detrital inputs and biogenic sources (Thompson and Oldfield, 1986; Liu et al., 2012). A bilogarithmic plot of χ_{ARM}/χ versus χ_{ARM}/χ_{fd}% to identify the different sources of magnetic minerals was proposed (Oldfield, 1994). Higher χ_{ARM}/χ versus χ_{ARM}/χ_{fd}% values, especially χ_{ARM}/χ_{fd}% >1.0×10³ indicated that magnetite was derived from biogenic sources. In this study, the χ_{ARM}/χ values range from 8.5 to 13.2, with a mean of 10.8, and the χ_{ARM}/χ_{fd}% values range from 69.7 to 121.9, with a mean of 94.3, suggesting that magnetic minerals of core M5 in the Bohai Sea can primarily be attributed to detrital input. In addition, the previous studies show that χ vs. χ_{fd}% and χ vs. χ_{ARM}/χ were used to differentiate the magnetic minerals generated
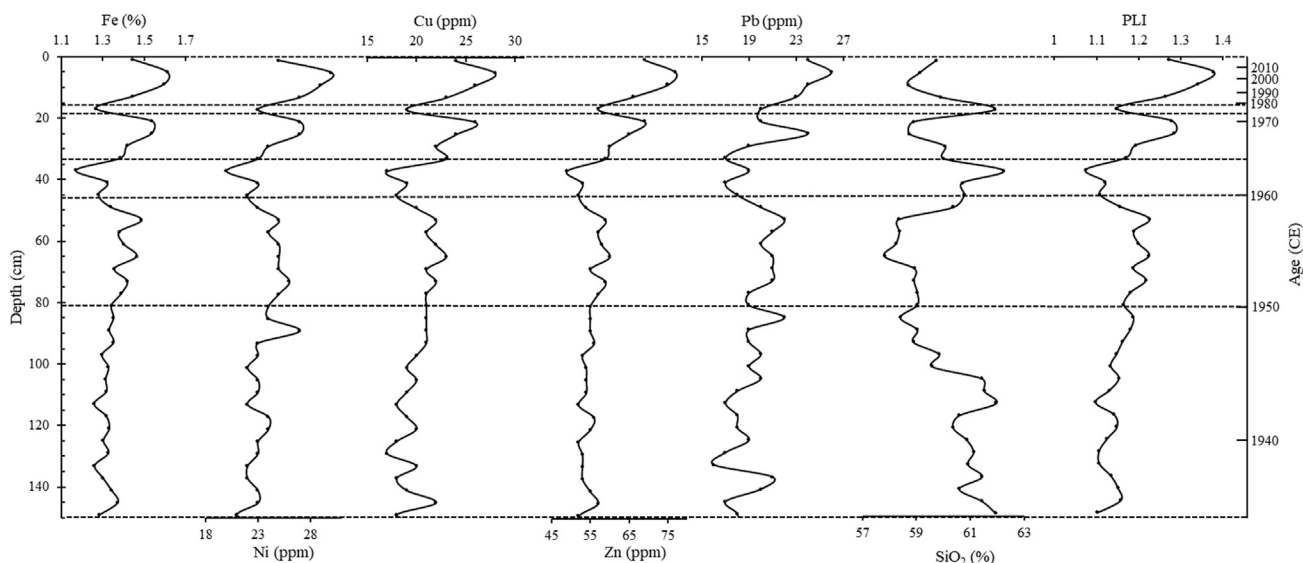
Figure 4. Heavy metals including Fe, Ni, Cu, Zn, Pb, and SiO₂, PLI against depth

from anthropogenic activities (Ma et al., 2014; Wang et al., 2018a, 2018b). In this study, the relationship between χ and χ_{fd}% and χ_{ARM}/χ can be divided into two parts. The pollution level of samples from the bottom to a depth of 81 cm is the lowest as shown by the heavy metal contents and the PLI curves. This indicates that the surrounding catchment is the main source of the magnetic minerals (Wang et al., 2018a, 2018b). The samples in the upper 81 cm have serious pollution levels, which show more influence of human activity.

Correlation between magnetic parameters and heavy metal content

Previous studies have shown that there is a strong correlation between magnetic minerals and heavy metal content (Dong et al., 2014; Bandaru et al., 2016; Wang et al., 2018a, 2018b). The results of Pearson's correlation coefficients (R^2) between the magnetic parameters and heavy metal content of core M5 from the Bohai Sea are shown in Table 2. The results showed that χ, SIRM, and χ_{ARM} have significantly positive correlations with Fe, Ni, Cu, Zn, and Pb ($R^2 = 0.601–0.865$), which indicated that magnetic minerals and heavy metals have essential linkages of source, migration, and deposition. Furthermore, the R^2 values between the magnetic parameters and PLI fall in the range of 0.709–0.897, indicating that magnetic parameters can be used to assess heavy metal pollution in the Bohai Sea. There are slight correlations between the heavy metal content as well as χ_{fd}% and S_{-ratio}, indicating that heavy metal pollution is not caused by a single magnetic mineral.

Principal component analysis (PCA) can be used to reveal the relationships between magnetic minerals and heavy metals (Zhu et al., 2012; Wang et al., 2018a, 2018b). Table 3 shows that heavy metals and magnetic parameters account for three principal components, accounting for 89.229% of the total variance. PC1 accounted for 69.825% of the total variances and has higher loadings on χ, SIRM, χ_{ARM}, Fe, Cu, Zn, Ni, Pb, and PLI. PC2 accounted for 10.117% of the total variance with a loading of χ_{fd}%, and PC3 was related to S_{-ratio}, accounting for 9.287% of the total variance. These findings clearly revealed that χ_{fd}% and S_{-ratio} showed no correlation with χ, SIRM, χ_{ARM}, or heavy metal content.

Environmental implications of magnetic parameters and heavy metals

Since the Yellow River began to flow into the Bohai Sea in 1855, the sedimentary sources of the latter tended to be stable. Therefore, ^{210}Pb and ^{137}Cs dating methods can be used to construct the age model from 1855 (Figure 2). The sediment recording the history of anthropogenic metals is a valuable tool to understand the historic anthropogenic influences and to project the heavy metal contamination in the future, which is helpful to form government policies for pollution emissions. In this study, concentration-related magnetic parameters (χ, SIRM, and χ_{ARM}) and heavy metal content, including Fe, Cu, Zn, Ni, Pb, and PLI of core M5 from the Bohai Sea, began to increase significantly at a depth of 81 cm (Figure 3). Combined
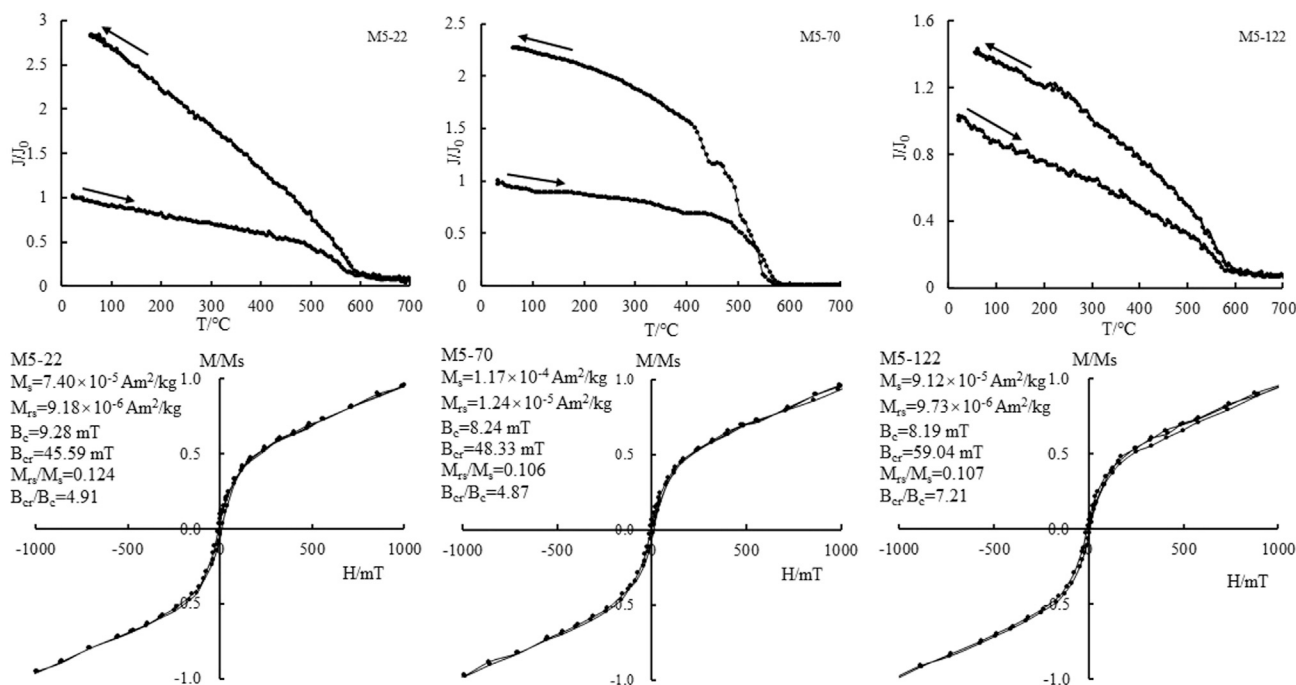
Figure 5. High-temperature κ-T curves and magnetic hysteresis loops for representative samples of core M5 from the Bohai Sea

with the ^{210}Pb and ^{137}Cs data, the age at a depth of 81 cm was placed at 1950 CE, which corresponded to the establishment of the People's Republic of China. With China's establishment, the steel production increased significantly due to the needs of social development, resulting in the increase in the magnetic parameters and heavy metals of core M5 (Editorial Committee of China Iron and Steel Industry ECCISI, 2018). All these indicated that modern industries became the dominant factor for heavy metal pollutions. Moreover, the χ, SIRM, and χ$_{ARM}$ values as well as heavy metal content and PLI of core M5 show an obvious decrease at a depth of 37–45 cm (Figure 3), corresponding to 1960–1962 CE. With the end of the Great Leap Forward at 1960 CE, the eight-character policy was suggested and the production of steel was decimated. The national steel output shrank from 13.51 million tons in 1960 CE to 6.67 million tons in 1962 CE with a reduction rate of 50.63% (Editorial Committee of China Iron and Steel Industry ECCISI, 2018). All the changes were recorded by the χ, SIRM, and χ$_{ARM}$ values as well as heavy metal content and PLI of core M5. Meanwhile, the decrease in concentration-related magnetic parameters, heavy metal content, and PLI at a depth of 16–18 cm was dated to 1976 CE, which corresponded to the Tangshan Earthquake of 1976 CE (Figure 3). Earthquakes have been studied using magnetic characteristics. Previous studies have shown that more clastic sediments were produced when earthquakes occurred (Yang et al., 2012; Zhang et al., 2017), which were also confirmed by the decrease of the grain size of the sediments. When the Tangshan earthquake occurred, more silicates from the Bohai Sea Rim deposited into the Bohai Sea, which was also supported by the increase in SiO$_2$ (Figure 3). SiO$_2$ is diamagnetic, and its susceptibility values are negative (Wang et al., 2017a, 2017b). The entry of SiO$_2$ lead to a decrease in the χ, SIRM, and χ$_{ARM}$ values of core M5 at a depth of 17 cm. Moreover, the entry of a large amount of SiO$_2$ diluted the heavy metal content of sediments of core M5, resulting in their reduction.

Limitations of the study

The results of this study indicate that the mineral magnetic method remains a promising tool in sediment pollution studies. However, its application as proxy of heavy metal concentrations needs careful consideration. First, magnetic minerals in sediments are derived from lithogenic, pedogenic, and anthropogenic sources. Therefore, it is necessary to disentangle these signals for the best application of the technique. Second, even when magnetic mineral particles are primarily derived from anthropogenic sources, the linkage with heavy metals is still poorly understood. Some heavy metals may have a common source with magnetic particles, while others may not. Third, hydrodynamic sorting effects along the source-to-sink pathway can alter the linkage between magnetic minerals and heavy metals. A number of studies have shown that
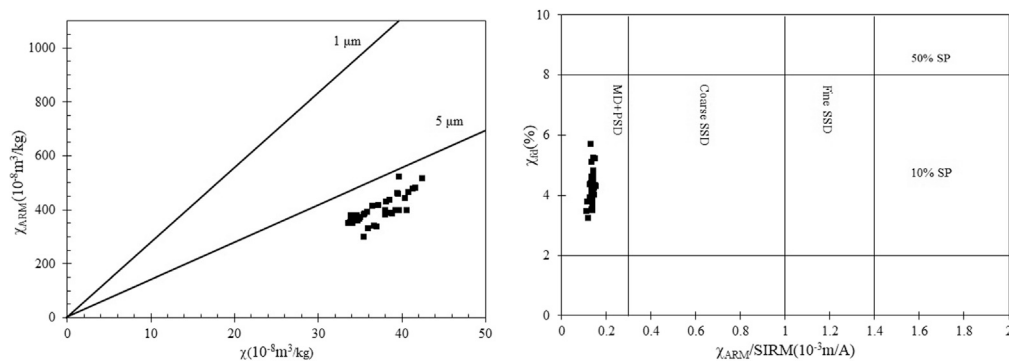
Figure 6. King plot (left) and Dearing diagrams (right) of the sediments of core M5 from the Bohai Sea

sorting can lead to the selective transport of magnetic minerals. In the future development of using the environmental magnetic parameters to monitoring heavy metal pollution, more efforts should be made to explore the new significance and magnetic mechanism of existing magnetic parameters, and find new environmental magnetic parameters (Zhang et al., 2018).

Conclusions

According to magnetic parameters, the heavy metal concentrations of Fe, Cu, Zn, Ni, Pb, and PLI, this study indicated the coexistence of magnetic parameters and heavy metals in sediments of core M5 from the Bohai Sea. The concentration-related magnetic parameters (χ, SIRM, and χ_{ARM}), heavy metal concentrations, and PLI increased at a depth of 81 cm and showed two obvious reductions at depths of 16–18 cm and 37–45 cm. Rock magnetic measurements demonstrated that the predominant magnetic mineral of core M5 was magnetite. Pearson correlation analysis and PCA showed that the χ, SIRM, and χ_{ARM} values as well as heavy metal content and PLI indicated that there were essential linkages of the sources, migration, and deposition between the magnetic particles and heavy metals. χ, χ_{ARM}, and SIRM can be used to assess heavy metal pollution. Using chronological data based on ^{210}Pb and ^{137}Cs activities, the increase in concentration-related magnetic parameters, heavy metals content, and PLI at the depth of 81 cm was dated to 1950 CE, corresponding to the establishment of the People's Republic of China, and the reduction at depths of 37–45 cm and 16–18 cm may be related to the decline of steel production in 1960 CE and the Tangshan earthquake in 1978 CE, respectively.

STAR★METHODS

Detailed methods are provided in the online version of this paper and include the following:

- KEY RESOURCES TABLE
- RESOURCE AVAILABILITY
  - Lead contact
  - Materials availability
  - Data and code availability
- METHOD DETAILS
  - Radiometric ^{210}Pb and ^{134}Cs
  - High- and low-frequency magnetic susceptibility
  - Anhysteretic remanent magnetization
  - Isothermal remanent magnetization
  - Magnetic hysteresis loops
  - High-temperature κ–T curves
  - Heavy-metal measurement
- QUANTIFICATION AND STATISTICAL ANALYSIS

ACKNOWLEDGMENTS

	χ	SIRM	χ_{ARM}	χ_{fd}	S_{-ratio}	Fe	Ni	Cu	Zn	Pb	PLI
χ	1	0.876	0.802	0.520	0.174	0.712	0.651	0.676	0.635	0.601	0.709
SIRM		1	0.859	0.305	0.056	0.865	0.827	0.844	0.837	0.771	0.897
χ_{ARM}			1	0.419	0.069	0.849	0.814	0.786	0.783	0.665	0.838
χ_{fd}				1	0.084	0.342	0.365	0.294	0.124	0.141	0.272
S_{-ratio}					1	0.323	0.160	0.242	0.300	0.098	0.228
Fe						1	0.883	0.920	0.918	0.717	0.952
Ni							1	0.860	0.863	0.815	0.928
Cu								1	0.924	0.673	0.946
Zn									1	0.746	0.959
Pb										1	0.843
PLI											1

AUTHOR CONTRIBUTIONS

X.H.W. Conceptualization, methodology, writing - original draft. L.S.W. Data curation, writing-review & editing. S.Y.H. Data curation, writing-review & editing. L.W.M. Conceptualization, methodology, software.

Table 3. Principal component analysis results from magnetic parameters and heavy metals of the sediments of core M5 from Bohai Sea

	Components		
	PC1	PC2	PC3
χ	0.818	0.340	0.111
SIRM	0.940	0.094	−0.167
χ_{ARM}	0.902	0.200	−0.075
$\chi_{fd}\%$	0.381	0.767	0.439
S_{-ratio}	0.233	−0.460	0.843
Fe	0.959	−0.096	0.091
Ni	0.922	−0.009	−0.044
Cu	0.933	−0.116	0.013
Zn	0.929	−0.294	−0.037
Pb	0.806	−0.143	−0.239
PLI	0.981	−0.137	−0.062
Eigenvalues	7.681	1.113	1.022
% of variance	69.825	10.117	9.287
Cumulative %	69.825	79.941	89.229

REFERENCES

Appleby, P.G., and Oldfeld, F. (1978). The calculation of lead-210 dates assuming a constant rate of supply of unsupported 210Pb to the sediment. Catena *5*, 1–8.

Appleby, P.G., and Oldfeldz, F. (1983). The assessment of ^{210}Pb data from sites with varying sediment accumulation rates. Hydrobiologia *103*, 29–35.

Bandaru, V.L., Gawali, P.B., Hanamgond, P.T., and Kannan, D. (2016). Heavy metal monitoring of beach sands through environmental magnetism technique: a case study from Vengurla and Aravali beaches of Sindhudurg district, Maharashtra, India. Environ. Earth Sci. *75*, 678.

Chen, J., and Wang, F. (1996). Chemical composition of river particulates in eastern China. Geojournal *40*, 31–37.

Cui, S.X. (2015). Present Situation and Historical Evaluation of Regional Development Around Bohai Sea (Ocean Press). (in Chinese).

Dearing, J.A., Dann, R.J.L., Hay, K., Lees, J.A., Loveland, P.J., Maher, B.A., and O'Grady, K. (1996). Frequency-dependent susceptibility measurements of environmental materials. Geophys. J. Int. *124*, 228–240.

Deng, C., Zhu, R., Verosub, K.L., Singer, M.J., and Yuan, B. (2000). Paleoclimatic significance of the temperature-dependent susceptibility of Holocene Loess along a NW-SE transect in the Chinese Loess Plateau. Geophys. Res. Lett. *27*, 3715–3718.

Dong, C., Zhang, W., Ma, H., Feng, H., Lu, H., Dong, Y., and Yu, L. (2014). A magnetic record of heavy metal pollution in the Yangtze River subaqueous delta. Sci. Total Environ. *476–477*, 368–377.

Editorial Committee of China Iron and Steel Industry (ECCISI) (2018). Yearbook of Chinese Iron and Steel Industry (China Metallurgical Press).

Gao, X., Zhou, F., and Chen, C.T.A. (2014). Pollution status of the Bohai Sea: an overview of the environmental quality assessment related trace metals. Environ. Int. *62*, 12–30.

King, J., Banerjee, S.K., Marvin, J., and Özdemir, Ö. (1982). A comparison of different magnetic methods of determining the relative grain size of magnetite in natural materials: some results from lake sediments. Earth Planet Sci. Lett. *59*, 404–419.

Leslie, C., and Hancock, G.J. (2008). Estimating the date corresponding to the horizon of the first detection of ^{137}Cs and $^{239+240}$Pu in sediment cores. J. Environ. Radioact. *99*, 483–490.

Li, H., Qian, X., Wei, H., Zhang, R., Yang, Y., Liu, Z., Hu, W., Gao, H., and Wang, Y. (2014). Magnetic properties as proxies for the evaluation of heavy metal contamination in urban street dusts of Nanjing, Southeast China. Geophys. J. Int. *199*, 1354–1366.

Li, S., and Zhang, Q. (2010). Spatial characterization of dissolved trace elements and heavy metals in the upper Han River (China) using multivariate statistical techniques. J. Hazard Mater. *176*, 579–588.

Liu, J.G., Li, A.C., Chen, M.H., and Xu, F.J. (2007). Geochemical characteristics of sediments in the Bohai mud area during Holocene. Geochimica *36*, 633–637.

Liu, Q., Roberts, A.P., Larrasoaña, J.C., Banerjee, S.K., Guyodo, Y., Tauxe, L., and Oldfield, F. (2012). Environmental magnetism: principles and applications. Rev. Geophys. *50*, RG4002.

Ma, M.M., Hu, S.Y., Lin, H., Cao, L.W., and Wang, L.S. (2014). Magnetic responses to traffic related contamination recorded by backfills: a case study from Tongling City, China. J. Appl. Geophys. *107*, 119–128.

Mariyanto, M., Amir, M.F., Utama, W., Hamdan, A.M., Bijaksana, S., Pratama, A., Yunginger, R., and Sudarningsih, S. (2019). Heavy metal contents and magnetic properties of surface sediments in volcanic and tropical environment from Brantas River, Jawa Timur Province, Indonesia. Sci. Total Environ. *675*, 632–641.

Oldfield, F. (1994). Toward the discrimination of fine-grained ferrimagnets by magnetic measurements in lake and near-shore marine sediments. J. Geophys. Res. *99*, 9045–9050.

Peters, C., and Dekkers, M.J. (2003). Selected room temperature magnetic parameters as a function of mineralogy, concentration and grain size. Phys. Chem. Earth Parts A/B/C *28*, 659–667.

Qiao, S., Shi, X., Zhu, A., Liu, Y., Bi, N., Fang, X., and Yang, G. (2010). Distribution and transport of suspended sediments off the Yellow River (Huanghe) mouth and the nearby Bohai Sea. Estuar. Coast Shelf Sci. *86*, 337–344.

Sagnotti, L., and Winkler, A. (2012). On the magnetic characterization and quantifcation of the superparamagnetic fraction of trafc-related urban airborne PM in Rome. Atmos. Environ. *59*, 131–140.

State Oceanic Administration of China (2014). China Marine Environmental Quality Bulletin in 2013 (China Oceanic Information Network).

Thompson, R., and Oldfield, F. (1986). Environmental Magnetism (Allen and Unwin).

Thompson, R., Stober, J.C., Turner, G.M., Oldfield, F., Bloemendal, J., Dearing, J.A., and Rummery, T.A. (1980). Environmental applications of magnetic measurements. Science *207*, 481–486.

Wang, G., Liu, Y., Chen, J., Ren, F., Chen, Y., Ye, F., and Zhang, W. (2018a). Magnetic evidence for heavy metal pollution of topsoil in Shanghai, China. Front. Earth Sci. *12*, 125–133.

Wang, H., Wu, X., Bi, N., Li, S., Yuan, P., Wang, A., Syvitski, J.P., Saito, Y., Yang, Z., Liu, S., and Nittrouer, J. (2017a). Impacts of the dam-orientated water-sediment regulation scheme on the lower reaches and delta of the Yellow River (Huanghe): a review. Global Planet. Change *157*, 93–113.

Wang, L., Hu, S., Ma, M., Wang, X., Wang, Q., Zhang, Z., and Shen, J. (2018b). Responses of magnetic properties to heavy metal pollution recorded by lacustrine sediments from the Lugu Lake, Southwest China. Environ. Sci. Pollut. Res. Int. *25*, 26527–26538.

Wang, L., Hu, S., Ma, M., Zhang, Y., Wang, X., Wang, Q., Zhang, Z., Cui, B., and Liu, X. (2019). Magnetic characteristics of atmospheric dustfall in a subtropical monsoon climate zone of China and its environmental implications: a case study of Nanjing. Atmos. Environ. *212*, 231–238.

Wang, L., Hu, S., Yu, G., Ma, M., and Liao, M. (2017b). Comparative study on magnetic minerals of tidal flat deposits from different sediment sources in Jiangsu coast, Eastern China. Stud. Geophys. Geod. *61*, 754–771.

Xu, L., Xu, X., and Meng, X. (2013). Risk assessment of soil erosion in different rainfall scenarios by RUSLE model

coupled with Information Diffusion model: a case study of Bohai Rim, China. Catena *100*, 74–82.

Yang, T., Chen, J., Wang, H., and Jin, H. (2012). Rock magnetic properties of fault rocks from the rupture of the 2008 Wenchuan earthquake, China and their implications: preliminary results from the Zhaojiagou outcrop, Beichuan County (Sichuan). Tectonophysics *530–531*, 331–341.

Yu, X., and Lu, S. (2016). Multiscale correlations of iron phases and heavy metals in technogenic magnetic particles from contaminated soils. Environ. Pollut. *219*, 19–27.

Zhang, L., Sun, Z., Li, H., Zhao, L., Song, S.R., Chou, Y.M., Cao, Y., Ye, X., Wang, H., and He, X. (2017). Rock record and magnetic response to large earthquakes within Wenchuan Earthquake Fault Scientific Drilling cores. Geochem. Geophys. Geosyst. *18*, 1889–1906.

Zhang, W., Dong, C., Hutchinson, S.M., Ge, C., Wang, F., and Feng, H. (2018). Recent applications of mineral magnetic methods in sediment pollution studies: a review. Curr. Pollut. Rep. *4*, 1–7. https://doi.org/10.1007/s40726-018-0075-y.

Zhao, B.R., Zhuang, G.W., Cao, D.M., and Lei, F.H. (1995). Circulation, tidal residual currents and their effects on the sedimentation in the Bohai Sea. Oceanol. Limnol. Sin. *26*, 466–473.

Zhou, L., Shi, Y., Zhao, Y., Yang, Y., Jia, J., Gao, J., Wang, Y.P., Li, Z., Zhang, Y., Guo, Y., et al. (2021). Extreme floods of the Changjiang River over the past two millennia: contributions of climate change and human activity. Mar. Geol. *433*, 106418.

Zhu, Z., Han, Z., Bi, X., and Yang, W. (2012). The relationship between magnetic parameters and heavy metal contents of indoor dust in e-waste recycling impacted area, Southeast China. Sci. Total Environ. *433*, 302–308.

STAR★METHODS

KEY RESOURCES TABLE

REAGENT or RESOURCE	SOURCE	IDENTIFIER
Deposited data		
China's Soil Science Database	Institute of Soil Science, Chinese Academy of Sciences	http://vdb3.soil.csdb.cn/
Software and algorithms		
SPSS/window	Statistical software for data science	Version 20, IBM

RESOURCE AVAILABILITY

Lead contact

Further information and resource requests should be directed to the lead contact: Longsheng Wang (52wls@163.com).

Materials availability

This study did not generate new unique materials.

Data and code availability

- Magnetic and heavy-metal data reported in this paper is available in Figures 3 and 4 and Table 1. All data reported in this paper will share by the lead contact on request.

- This paper does not report original code.

- Any additional information required to reanalyze the data reported in this paper is available from the lead contact on request.

METHOD DETAILS

Radiometric ^{210}Pb and ^{134}Cs

The chronology of core M5 was established using radiometric ^{210}Pb and ^{134}Cs dating over a depth of 0–150 cm. Each sample was sealed in a plastic box for a month, reaching radioactive equilibrium after being dried and powdered. The total ^{210}Pb activity was attained at 46.5 keV, and ^{137}Cs activity was measured from a γ-ray peak at 661.6 keV. ^{226}Ra activity was measured using γ radiation of 609.3 keV (^{214}Bi) and 351.9 keV (^{214}Pb). ^{210}Pbexc activity was calculated by subtracting the ^{226}Ra activity from the total ^{210}Pb activity. The average sedimentation rate was calculated using the constant initial concentration model (Appleby and Oldfeld, 1978; Appleby and Oldfeldz, 1983). ^{210}Pb and ^{137}Cs was measured at East China Normal University.

High- and low-frequency magnetic susceptibility

High- and low-frequency magnetic susceptibility (χ_{hf} and χ_{lf}) was measured using a Bartington MS2B susceptibility meter, and frequency susceptibility was calculated using the formula $\chi_{fd}\% = ((\chi_{lf} - \chi_{hf})/\chi_{lf}) \times 100$.

Anhysteretic remanent magnetization

Anhysteretic remanent magnetization (ARM) was imparted with a peak AF field of 100 mT and a DC bias field of 0.05 mT using a Molspin alternating field demagnetiser, and then measured with a Molspin Minispin magnetometer.

Isothermal remanent magnetization

Isothermal remanent magnetization (IRM) was imparted using an ASC IM-10-30 pulse magnetizer and measured using the Molspin Minispin magnetometer. The IRM at 2.5 T was considered to be the saturation isothermal remanent magnetization (SIRM). Backfield remagnetization of IRM was measured at −300 mT using the reverse fields (IRM$_{-300\ mT}$), and calculated S$_{-ratio}$ by IRM$_{-300\ mT}$/SIRM.

Magnetic hysteresis loops

Magnetic hysteresis loops were measured using variable field translation balance with a maximum field intensity of 1,000 mT.

High-temperature κ–T curves

High-temperature κ–T curves were carried out using a KLY-3 Kappabridge attached to a CS-3 high-temperature device in air.

Heavy-metal measurement

The concentration of heavy metals was determined by wavelength dispersive X-ray fluorescence spectrometry (XRF, PANalytical PW2403) with a detection limit of 0.1 mg/kg. Blank, standard (GSS4, GSR5, GSD3), and repeated samples were analyzed simultaneously in the experiment to provide a basis for quality control. With relative standard deviation as the standard, the analytical precision was 3–5%. The accuracy of the analysis was checked using standard and duplicate samples. The quality control provided good precision (S.D. < 5%).

QUANTIFICATION AND STATISTICAL ANALYSIS

To accurately indicate the pollution level, we calculated the Tomlinson pollution load index (PLI) as follows: $PLI_z = (CF_{1z} \times CF_{2z} \times \ldots \times CF_{nz})1/n$, and $CF_z = C_{mz}/C_{bg}$; where z is depth of the samples, CF_z is the respective heavy metal concentration factor, C_{mz} is the concentration of heavy metal, C_{bg} is the respective heavy metal mean background concentration. C_{bg} were derived from the average values of heavy metals from the bottom to a depth of 81 cm before pollution.

Pearson correlation analysis and principal component analysis were performed using the commercial statistics software package SPSS version 20 for Windows.